EULERIAN MEAN VELOCITIES UNDER NON-BREAKING WAVES ON HORIZONTAL BOTTOMS

Peter Nielsen[1] & Zai-Jin You[2]

Abstract

A model is presented for the Eulerian time-mean velocities in combined wave-current flows. The typical, measured profiles of weak currents are well modelled. This includes the "toe" of forward drift in the wave boundary layer and the very flat (as opposed to the parabolic shape of laminar models) current profile between the bottom boundary layer and the wave trough. The model relies on a local force balance like Longuet-Higgins' (1953) diffusion solution rather than on advective influence from the end conditions. This seems justified by experiments, probably because a sufficient amount of turbulent diffusivity is present even for very weak currents. In its present form the model can only handle currents which are so weak that their influence on the wave motion is negligible. However, agreement with measurements of stronger currents can be obtained by modification of the wave Reynolds stress to account the influence of the current on the wave motion. Application to surf zone conditions also require modifications, but the essential structure of the model is globally applicable.

Introduction

Several authors eg. van Doorn & Godefroy (1978), van Doorn (1981), Kemp & Simons (1982), Kaaij & Nieuwjaar (1987), Kampen & Nap (1988), Heiboer (1988), Villaret & Perrier (1992) and Klopman (1994) have found that Eulerian mean velocities under progressive, non breaking waves show different distributions from what has been expected. Following currents reach a maximum value and subsequently decrease towards the surface. See Figure 1. The trend is found for all current strengths as long as the time averaged bed shear stress is in the direction of wave propagation $\left(d\overline{u}/dz > 0 \text{ for } z \to 0^+\right)$ but is not found for currents in the opposite direction. Opposing currents show the oppostive anomaly. That is, compared with a logarithmic profile, the opposing current grows more rapidly towards the surface.

----

[1] Reader, Department of Civil Engineering, University of Queensland AUSTRALIA 4072, Fax +61 7 3365 4599, [2] Victorian Institute of Marine and Freshwater Resources.

4066

Thus, observations of both following and opposing currents contrast with the existing simple wave current boundary layer models, e g, Grant and Madsen (1979), Fredsoe (1984), Coffey & Nielsen (1986) or You (1994) which all predict logarithmic, i e, monotonically increasing current velocities above the wave boundary layer.

It is obvious from Figure 1 that the depth averaged current velocity $< \bar{u} >$ may be significantly overpredicted by the old type of models for following currents. The elevation at which the current maximum occurs depends on the relative strength of the current. For very weak currents, eg. flume experiments with zero net flow, it occurs very close to the bed, i e, below or near the top of the wave boundary layer. For stronger currents, it occurs closer to the mean water surface. This trend was clearly shown by the measurements of Kemp and Simons (1982). The data in Figure 1 were obtained over a fixed bed but numerous profiles over sand beds, measured by Heijboer (1988) and Villaret & Perrier (1992) show the same trends.
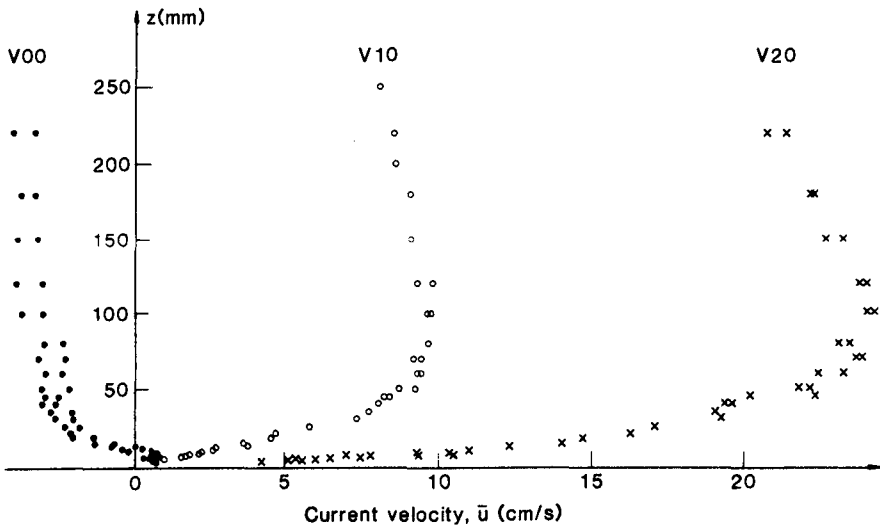

Figure 1: Eulerian mean velocities measured under non breaking waves. van Doorn (1981) test V00, V10, V20. In all tests the wave parametres were $(D,T,H,)=(0.3m, 2.0s, 0.12m)$, and the bed roughness was artificial ripples with Nikuradse roughness $r = 2.1cm$.

The current maximum is not seen in velocity profiles from U-tube experiments like those of van Doorn (1983). It was therefore suggested by Nielsen (1992) that the profile type in Figure 1 can be understood in terms of the wave Reynolds stress $-\rho \widetilde{u}\widetilde{w}$ which exist under a progressive wave with a bottom boundary layer but not in the U-tubes. The tilde indicates periodic components with zero mean, corresponding to the definition $u(t) = \bar{u} + \tilde{u}(t) + u'(t)$.

Figure 2 shows corresponding examples of following and opposing currents superimposed on the same waves (same period and same wave height) measured by Klopman (1994). Klopman's data show very clearly the difference in profile shape

caused by the wave Reynolds stress $-\rho\overline{\tilde{u}\tilde{w}}$. Wave basin measurements by Havinga (1992) with angles of 60°, 90° and 120° between current and wave propagation show intermediate stages of this phenomenon.

The following outlines a model of current profiles in the presence of waves which takes $-\rho\overline{\tilde{u}\tilde{w}}$ into account explicitly in order to explain the shape of the velocity profiles in Figures 1 and 2. The model can successfully predict the distributions of weak currents as in a flume with no recirculation. For strong currents adjustments are needed to the distribution of $-\rho\overline{\tilde{u}\tilde{w}}$ which are as yet not understood. They are most likely due to non linear wave current interaction.
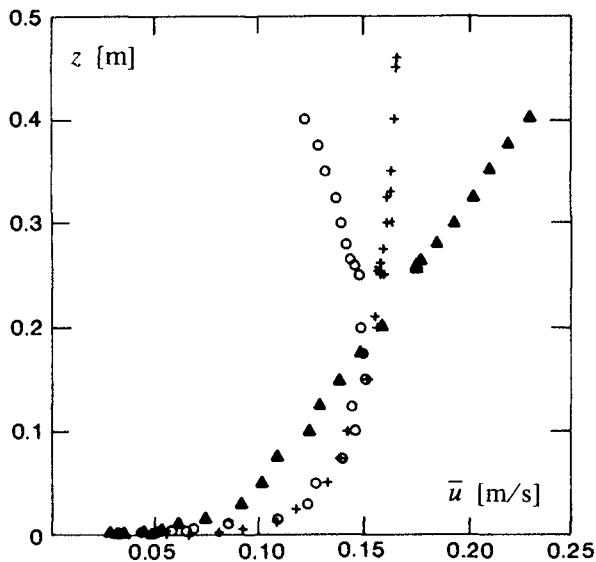

Figure 2: Current profiles in the presence of no waves (+), following waves (o) and opposing waves (triangle) of the same size. Depth $D = 0.5$m, wave period $T = 1.4$s and wave height $H = 0.12$m. After Klopman (1994).

Shear Stresses and Shear
In the following the notation of Nielsen (1992) will be followed. Thus, the symbol τ represents the total shearing force per unit area of a cross section or the total transfer of x-momentum in the z direction. Hence, in a two dimensional flow with steady, periodic and random velocity components $(u,w) = (\overline{u} + \tilde{u} + u', \overline{w} + \tilde{w} + w')$ in the x and z directions we have

$$\overline{\tau} = \rho\nu\frac{d\overline{u}}{dz} - \rho\overline{uw} = \rho\nu\frac{d\overline{u}}{dz} - \rho\,\overline{u}\,\overline{w} - \rho\overline{\tilde{u}\tilde{w}} - \rho\overline{u'w'} \qquad (1)$$

where, as usual, ν is the kinematic viscosity and ρ is the fluid density. The total normal stress (positive as tension) or horizontal transfer of x-momentum is corresponding given by

$$\overline{\sigma} = -\overline{p} - \rho\overline{u^2} + \rho\nu\frac{\partial\overline{u}}{\partial x} = -\overline{p} - \rho\overline{u}^2 - \rho\overline{\tilde{u}^2} - \rho\overline{u'^2} + \rho\nu\frac{\partial\overline{u}}{\partial x} \qquad (2)$$

and these two satisfy

$$\frac{\partial \overline{\tau}}{\partial z} + \frac{\partial \overline{\sigma}}{\partial x} = 0 \tag{3}$$

in a steady, two dimensional flow, i e,

$$\frac{\partial}{\partial z}\left[\nu\frac{d\overline{u}}{dz} - \overline{uw} - \overline{\widetilde{u}\widetilde{w}} - \overline{u'w'}\right] = \frac{\partial}{\partial x}\left[\frac{\overline{p}}{\rho} + \overline{u}^2 + \overline{\widetilde{u}^2} + \overline{u'^2} - \nu\frac{\partial\overline{u}}{\partial x}\right] \tag{4}$$

Here we assume, for the situation of waves and a weak current, that the second term on the left can be neglected and that the first and the third term are dominant on the right hand side so that we have

$$\frac{\partial}{\partial z}\left[\nu\frac{d\overline{u}}{dz} - \overline{\widetilde{u}\widetilde{w}} - \overline{u'w'}\right] = \frac{\partial}{\partial x}\left[\frac{\overline{p}}{\rho} + \overline{\widetilde{u}^2}\right] \tag{5}$$

which is integrated with the bottom boundary condition $\overline{\tau}(0) = \overline{\tau}_o$ to give

$$\nu\frac{\partial\overline{u}}{\partial z} - \overline{\widetilde{u}\widetilde{w}} - \overline{u'w'} = \frac{\overline{\tau}_o}{\rho} + \int_o^z \frac{\partial}{\partial x}\left[\frac{\overline{p}}{\rho} + \overline{\widetilde{u}^2}\right]dz \tag{6}$$

Here we may write the first and third terms on the left in terms of a current eddy viscosity ν_c and solve for the current gradient

$$\frac{\partial\overline{u}}{\partial z} = \frac{1}{\nu_c}\left(\frac{\overline{\tau}_o}{\rho} + \int_o^z \frac{\partial}{\partial x}\left[\frac{\overline{p}}{\rho} + \overline{\widetilde{u}^2}\right]dz + \overline{\widetilde{u}\widetilde{w}}\right) \tag{7}$$

This equation will then directly give the current distribution by integrating with the boundary condition $\overline{u}(0) = 0$.

If the main emphasis is on the flow near the bed, it is justified to assume that the mean pressure is hydrostatic. However, in order to get a good representation of the flow closer to the surface it is necessary to use $\overline{p} = \rho g(\overline{\eta} - z) - \rho\overline{\widetilde{w}^2}$ in which case Equation (7) can be written.

$$\frac{\partial\overline{u}}{\partial z} = \frac{1}{\nu_c}\left(\frac{\overline{\tau}_o}{\rho} + g\frac{\partial\overline{\eta}}{\partial x}z + \int_o^z\left[\frac{\partial}{\partial x}\left(\overline{\widetilde{u}^2} - \overline{\widetilde{w}^2}\right)\right]dz + \overline{\widetilde{u}\widetilde{w}}\right) = \frac{1}{\rho\nu_c}\left(\overline{\tau}_o - \int_o^z\frac{\partial\overline{\sigma}}{\partial x}dz + \overline{\widetilde{u}\widetilde{w}}\right) \tag{8}$$

This general expression explains qualitatively the shape of the current profiles in Figure 1. For all three cases, $\overline{\tau}_o$ is positive and hence the current gradient is positive at the bed where the other terms are zero. Those terms will however grow in magnitude with increasing z and they are all initially negative for non-breaking waves over a horizontal bed. Thus, the right hand side and hence the current gradient will change sign at a certain level and the current velocity shows a maximum, see Figure 3.

The mean bed shear stress

The bed shear stress $\tau_o = \overline{\tau}(0)$ can be determined from

$$\tau_o = \tau_w - \rho g D\frac{d\overline{\eta}}{dx} - \frac{d S_{xx}}{dx} \tag{9}$$

where $\overline{\tau}_w$ is the time averaged wind stress, D is the local mean depth, $\overline{\eta}$ is the mean surface elevation and S_{xx} is the wave radiation stress in the direction of wave propagation calculated from a suitable wave theory.

The radiation stress term

Assuming linear wave theory, the radiation stress term of Equation (8) is evaluated as

$$\int_o^z \frac{\partial}{\partial x}\left[\overline{\tilde{u}^2} - \overline{\tilde{w}^2}\right]dz = \int_o^z \left[\frac{1}{2}\frac{\partial}{\partial x}\left(\frac{\pi H}{T\sinh kd}\right)^2 \left[\cosh^2 kz - \sinh^2 kz\right]\right]dz$$

$$= H\frac{dH}{dx}\frac{\pi^2}{T^2 \sinh^2 kd}\,z \qquad (10)$$

In general the wave height may also vary due to breaking, refraction, diffraction and shoaling, but if only bottom friction is important, the wave height gradient is given by

$$H\frac{dH}{dx} = -\frac{8}{3\pi g}\frac{f_e(A\omega)^3}{c_{g,r}+<\overline{u}>} \qquad (11)$$

where f_e is the energy dissipation factor ($\approx f_w$), $c_{g,r}$ is the wave group velocity relative to the current and $<\overline{u}>$ is the depth averaged current velocity. See e g Nielsen (1992) p 77. By inserting into (10) we obtain

$$\int_o^z \left[\frac{\partial}{\partial x}\left(\overline{\tilde{u}^2} - \overline{\tilde{w}^2}\right)\right]dz = \frac{-8\pi}{3\,g\,T^2 \sinh^2 kd}\frac{f_e(A\omega)^3}{c_{g,r}+<\overline{u}>}\,z \qquad (12)$$

Hence, the radiation stress contribution to the current shear in Equation (8) has the same form as the surface slope term, i e, both grow linearly in magnitude with distance from the bed. Consequently, the general picture which determines the level of the current maximum ($\frac{\partial \overline{u}}{\partial z} = 0$) is as shown in Figure 3. The current maximum occurs where the terms due to $\frac{\partial \overline{\sigma}}{\partial x}$ and $\overline{\tau}_w$ are balanced by the wave Reynolds stress.
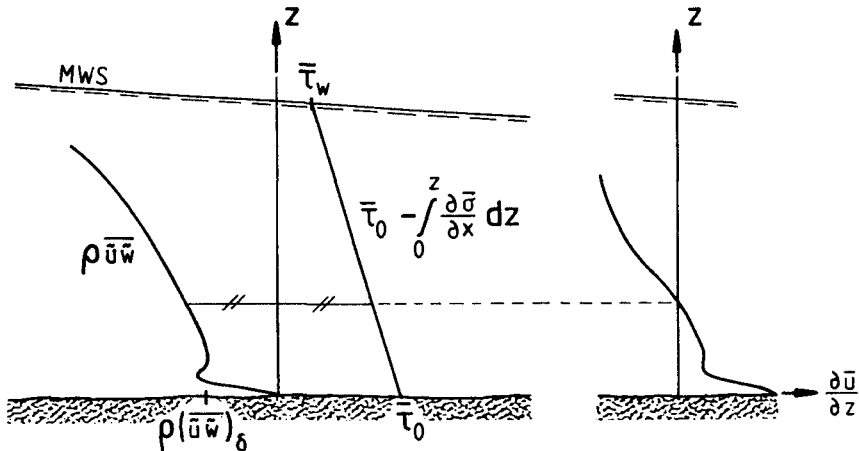

Figure 3: The current shear and the terms that generate it, cf Equation (8), for a typical situation of following current ($\overline{\tau}_o > 0$). The (lowest) current maximum will occur close to the bed for small $\overline{\tau}_o$ and closer to the MWS for larger $\overline{\tau}_o$, cf the measurements in Figure 1.

The wave Reynolds stress

The wave Reynolds stress $-\rho\overline{\tilde{u}\tilde{w}}$ may be seen as consisting of three components as shown by Bijker et al (1974). One due to the phase shifting of velocities in the boundary layer, one due to wave height decay and one due to bed slope.

Longuet-Higgins (1956) derived an expression for the first one for boundary layers with constant eddy viscosity. It varies through the wave boundary layer as

$$-\rho\overline{\tilde{u}\tilde{w}} = \rho\frac{1}{4}(A\omega)^2 k\delta\left[1 - e^{-\zeta}\left(2\cos\zeta - e^{-\zeta} + 2\zeta\sin\zeta\right)\right] \qquad (13)$$

where

$$\zeta = \frac{z}{\delta} = \frac{z}{\sqrt{2\nu_t/\omega}} \qquad (14)$$

Its asymptotic value above the boundary layer ($z \gg \delta$) is

$$-\rho\left(\overline{\tilde{u}\tilde{w}}\right)_\delta = -\rho\frac{1}{4}k\delta\ (A\omega)^2 \qquad (15)$$

which can be written in terms of the friction factor as

$$-\rho(\overline{\tilde{u}\tilde{w}})_\delta = \rho\frac{1}{4\sqrt{2}}\ k A^3 \omega^2\ f_w \qquad (16)$$

cf Nielsen (1992). The wave friction factor may be determined from

$$f_w = \exp\left[5.5\left(\frac{r}{A}\right)^{0.2} - 6.3\right] \quad \text{for } r/A < 1 \qquad (17)$$

as suggested by Nielsen (1992).

Estimation of $-\rho\overline{\tilde{u}\tilde{w}}$ in and above a turbulent boundary layer

The expression (13) was derived for wave boundary layers that are laminar or which are turbulent with constant eddy viscosity. For turbulent wave boundary layers with moderate relative roughness: $r/A < 0.06$ it is however necessary to adopt a different description, cf Nielsen 1992, p 47. At present we shall adopt the simple, boundary layer model of Nielsen (1985) by which the horizontal velocity under a decaying sine wave can be written as

$$\tilde{u}(z,t) = A\omega\left[\cosh kz - e^{-[1+i]\left(\frac{z}{z_1}\right)^p}\right]e^{i(\omega t - kx)} \qquad (18)$$

Provided the boundary layer is thin: $|kz_1| \ll 1$. The wave decay is described by the imaginary part of the wave number $k = k_r + ik_i$. We note that the wave decay is not exactly exponential for a turbulent boundary layer, but we have approximately

$$k_i = \frac{1}{H}\frac{dH}{dx} \approx -H\frac{8\pi^2}{3gT_a^3(c_{gr} + <\bar{u}>)\sinh^3 kd}f_e \qquad (19)$$

cf Nielsen (1992), p 78. T_a is the period seen by a fixed observer.

The boundary layer parameters z_1 and p may, for hydraulically rough (roughness r) conditions, be found from the following formulae from Nielsen (1985)

$$z_1 = 0.09\sqrt{r A} \qquad (20)$$

$$p = 0.59 \exp\left(0.59 \frac{1-(A/38r)^{1.8}}{1+(A/38r)^{1.8}} \right) \tag{21}$$

This model is likely to be satisfactory for all wave boundary layers in the relative roughness range which has so far been observed with beds of loose sand ($0.015 < r/A < 1$) as discussed by Nielsen (1992). For very rough beds, $p \to 1$, this model corresponds to constant eddy viscosity.

In order to find the wave reynolds stress $-\rho \overline{\tilde{u}\tilde{w}}$ we first find the vertical velocity that corresponds to (18) from the continuity principle:

$$\tilde{w} = \int_0^z -\frac{\partial \tilde{u}}{\partial x} dz = A\omega\, e^{i(\omega t - kx)} [i \sinh k\, z - ik \int_0^z e^{-(1+i)(\frac{z}{z_1})^p} dz] \tag{22}$$

where $\sinh kz \approx \sinh k_r z + i\, k_i z \cosh k_r z$ for $k_i z \ll 1$ so that

$$\tilde{w} \approx A\omega\, e^{i(\omega t - kx)} [-k_i z \cosh k_r z + i \sinh k_r z - ik \int_0^z e^{-(1+i)(\frac{z}{z_1})^p} dz] \tag{23}$$

Similarly the expression (18) for the horizontal velocity can be simplified to

$$\tilde{u} \approx A\omega\, e^{i(\omega t - kx)} [\cosh k_r z + ik_i z \sinh k_r z - e^{-(1+i)(\frac{z}{z_1})^p}] \tag{24}$$

Inside the boundary layer where $k_i z \ll k_r z \ll 1$ these expressions lead to an analogous (but very complicated) expression corresponding to (13). For the sake of brevity, we shall use (13) combined with (16) and with ζ replaced by $\xi = (z/z_1)^p$, i e,

$$(\overline{\tilde{u}\tilde{w}})_{BL} \approx -\frac{1}{4\sqrt{2}} k_r A^3 \omega^2 f_w \cosh k_r z \left[1 - e^{-\xi}\left(2\cos\xi - e^{-\xi} + 2\xi \sin\xi\right)\right] \tag{25}$$

where the subscript BL refers to this term being analogous to the boundary layer term considered by Longuet-Higgins (1956). The cosh factor only makes a difference far above the boundary layer where $\xi \gg 1$.

If we neglect the boundary layer terms (the last terms) in (22) and (23) we get the contribution due to wave decay:

$$(\overline{\tilde{u}\tilde{w}})_{DECAY} \approx -\frac{1}{2}(A\omega)^2 k_i z(\cosh^2 k_r z + \sinh^2 k_r z) = -\frac{1}{2}(A\omega)^2 k_i z \cosh 2k_r z \tag{26}$$

Figure 4 shows the two $\overline{\tilde{u}\tilde{w}}$-contributions, evaluated for Klopman's (1994) tests.
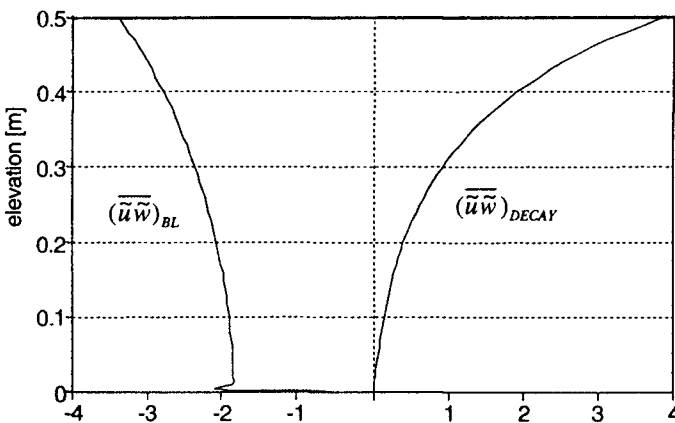
Figure 4: Wave Reynolds stress contributions for (h,T,H,r) = (0.5m, 1.4s, 0.12m, 0.0012m). The units are $m^2/s^2 \times 10^{-5}$.

The eddy viscosity distribution

In order to find the $\bar{u}$-distribution from Equation (8) we must specify the eddy viscosity $v_c(z)$ felt by the current. We use the distribution suggested by Nielsen (1992) which consists of a parabolic/constant part based on the current friction velocity $\bar{u}_* = \sqrt{\bar{\tau}_o / \rho}$ with a square toe added due to wave boundary layer mixing:

$$v_c(z) = Max \left\{ \begin{array}{c} 2\omega z_1^2 \\ 0.4\,\overline{u_*}z\left(1 - \frac{z}{D}\right) for\, z < D/2, \quad 0.1\overline{u_*}D \; for\; z > D/2 \end{array} \right\} \quad (27)$$

Discharge considerations

Calculation of the total discharge presents a problem because it must include the discharge which occurs above the wave trough where the velocities are not obtained by integration of Equation (8) as they are for the lower part of the flow. One estimate of the net flow between the wave trough and the crest can be obtained from linear wave theory namely

$$Q_{tc} = \frac{1}{8c} g H^2 \quad (28)$$

where c is the wave speed, see eg. Dean & Dalrymple (1991). It is however not obvious how this irrotational result can be combined with an integral over the lower flow domain ($z<D-H/2$) of the velocities obtained from Equation (8).

Identification	Q_{tc} [m²/s] based on Eq (28)	Measured $D-H/2$ $\int_{o} \bar{u}dz$ [m²/s]	Measured total Q [m²/s]	Total Q [m²/s] based on Eq (29)
Klopman 1994	0.010	-0.012	0	-0.06
" - ": monocrom, following	0.010	0.057	0.080	0.080
" - ": monocrom, opposing	0.010	-0.071	-0.080	-0.091
van Doorn & Godefroy, smooth	0.011	-0.0042	0	0.005
van Doorn & Godefroy, rough	0.011	-0.0062	0	0.001
van Doorn V00	0.011	-0.0073	0	0.0004
van Doorn V10	0.011	0.020	0.030	0.041
van Doorn V20	0.011	0.051	0.060	0.087

Table 1

We shall adopt the approach which is illustrated in Figure 5. That is, velocities below the wave trough are found from integration of Equation (8). Above the trough a parabolic velocity distribution corresponding to the flow rate given by Equation (28) is added to the velocity $\overline{u}_{tr}$ at the trough level. The total flow rate is then

$$Q = \int_{o}^{D-H/2} \bar{u}dz + \frac{gH^2}{8c} + \overline{u}_{tr}H \quad (29)$$

Some comparison between this approach and measurements is afforded by Table 1. There is obviously some scope for improvement but the message from this limited data set is not very clear.

The surface slope

The surface slope $d\overline{\eta}/dx$, albeit very small influences the current distribution and hence the net flow rate per unit width Q. Hence, it is not possible to achieve agreement with experiments if the surface slope is assumed to be zero. Not even for a "no current situation".

In practical applications it is some times Q which is specified while $d\overline{\eta}/dx$ is not. In such cases the model is easiest applied by trial and error. That is,

1. A reasonable value of $d\overline{\eta}/dx$ is guessed
2. Q is found by integrating Equation (8) and applying (29) to find Q.
3. An improved value of $d\overline{\eta}/dx$ is adopted.

The "necessary" surface slopes to match the usual wave flume conditions with horizontal beds are usually inside the range $\pm 5 \times 10^{-5}$. They are thus hardly measureable.

Comparison with experiments

A comparison of the model above with the "monocromatic waves, no current" experiment of Klopman (1994) is shown in Figure 5.
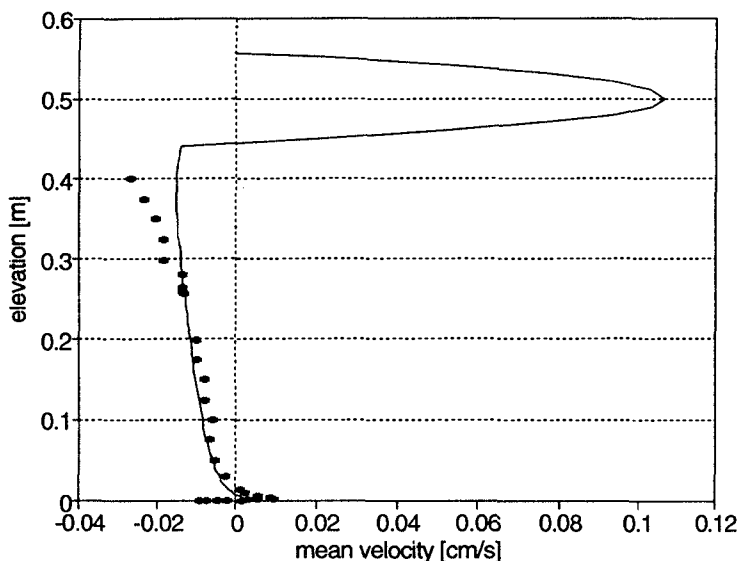

Figure 5: Model comparison with Klopmans data, Monocromatic waves, D=0.5m, T=1.4s, H=0.12m, Q=0m²/s. The flume bed was covered with a single layer of 2mm sand giving a Nikuradse roughness of r=1.2mm. In order to achieve zero nett flow with the model, a surface slope of 0.0000017 must be assumed.

Figure 5 shows some discrepancy between the model and the measurements below $z = 6$mm. Part of this might be corrected by making adjustments to the eddy viscosity distribution in this area. However, the existing detailed data sets: van Doorn & Godefroy (1978), van Doorn (1981), Swan (1990) and Klopman (1994) show quite some variation. In particular, the negative velocities measured by Klopman at $z <$ 1mm are not parallelled by the other experiments. At any rate, comparison is very great detail is not warranted at levels smaller than the roughness height between this model, which is horizontally uniform, and measurements which, at this level, will depend upon the horizontal position of the probe. Measurements may show horizontal variation both on the scale of individual roughness elements and on the scale of the wave length if some reflection and/or circulation cells occur in the flume.

While the agreement between the model and experiments with weak currents is good as shown by Figure 5, adjustments are necessary in order to model stronger currents. In general the data show a stronger deviation from the logarithmic profile than the model predicts. See Figure 6.
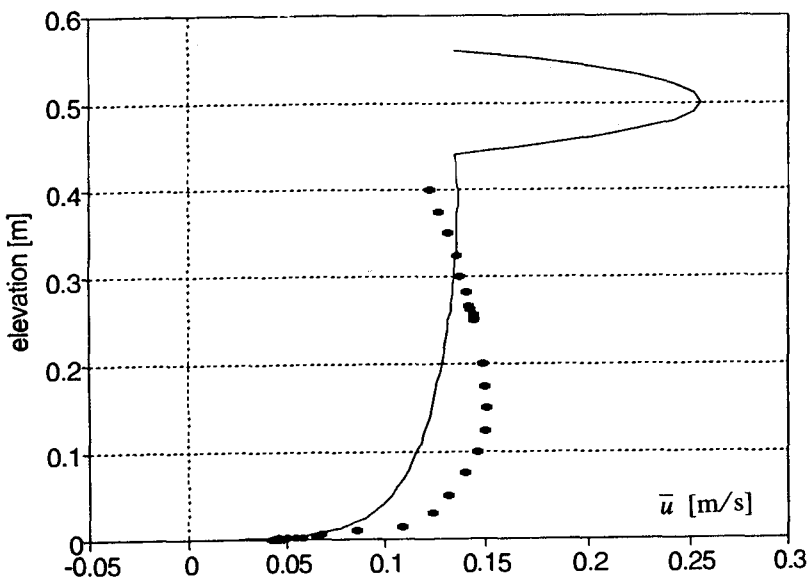

Figure 6: Comparison between the model and the "monocromatic waves, following current" experiment of Klopman (1994). $D=0.5$m, $T=1.4$s, $H=0.12$m, $Q=0.08$m^2/s, $r=1.2$mm. Surface slope -0.00000145.

Figure 6 shows a clear discrepancy between the model described above and Klopman's "following current" experiment. The reason is believed to be that this rather strong current ($< \bar{u} >= 0.92 A\omega$) changes the wave motion and hence $\overline{\tilde{u}\tilde{w}}$ in the upper part of the flow. An indication of this change can also be found the direct $\overline{\tilde{u}\tilde{w}}$ - measurements of Supharatid et al (1992).

Figure 7 shows an improved model performance obtained by enhancing the wave Reynolds stress component ($\overline{\tilde{u}\tilde{w}}$)$_{BL}$ (Equation 25) by the empirical factor

$$C_{WR} = 1 + 100 \frac{u_*}{A\omega} \frac{z}{D} \tag{30}$$

while ($\overline{\tilde{u}\tilde{w}}$)$_{DECAY}$ is kept unchanged.

This is a purely empirical adjustment but it is thought to mimic changes to $\overline{\tilde{u}\tilde{w}}$ in the upper part of the flow due to extra vorticity of the wave motion caused by interaction with the strong current. There is little reason to believe that $\overline{\tilde{u}\tilde{w}}$ is changed appreciably inside the wave boundary layer by the current, cf the data Supharatid et al (1992) and Nielsen (1985, 1992). It is noted, however, that the same empirical adjustment would also improve the agreement with the zero-net-flow-data in Figure 5.
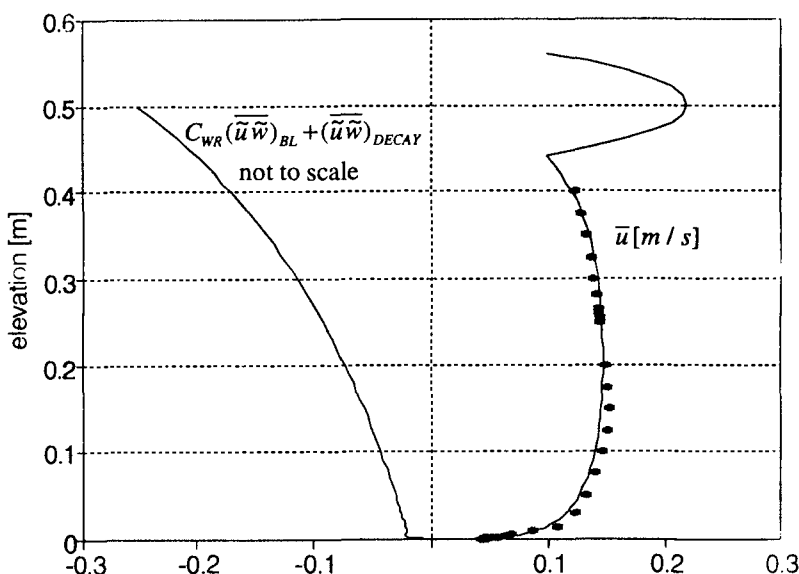

Figure 7: Comparison of the model with empirically enhanced wave Reynolds stress to the same data as in Figure 6. Surface slope -0.000021. The curve on the left shows the enhance distribution of $\overline{\tilde{u}\tilde{w}}$ given by Equations (25), (26) and (30).

Discussion

The magnitude of the eddy viscosity and its capacity to transfer vorticity upwards from the bed influences the nature of the solution as discussed by Longuet-Higgins (1953). If the eddy viscosity is small, the $\overline{u}$-profile would be strongly influenced by the end conditions through horizontal advection. In that case it would not be determined from the local force balance which leads to Equation (8). However Euation (35) leads to eddy viscosities which are very much larger than the laminar viscosity even in the "no current situations" corresponding to Figure 1a and Figure 4. Thus, in Klopman's "no current" experiment Equation (9) gives a bed shear stress of

$0.015 N/m^2$ corresponding to an eddy viscosity at mid depth of $0.00039 m^2/s$, about four hundred times the laminar viscosity. This is probably the reason why "no current" experiments quite consistently show $\bar{u}$-profiles like to ones in Figure 1a and Figure 5 even thogh they may have different end conditions.

In other words, it appears that under conditions like those of van Doorn (1981) and Klopman (1994) and even the smooth bed experiments of van Doorn & Godefroy (1978) $(D,T,H) = (0.3m, 2s, 0.12m)$ the eddy viscosity is strong enough that the net flow is governed by the local conditions as expressed by Equation (8). The experimental conditions of Swan (1990), smooth bed and $(D,T,H) =$ (0.369m, 0.893s, 0.06m) are probably close to the limit although he did show (his Figure 5a) a $\bar{u}$-profile which is qualitatively similar to those observed under more vigorous flow conditions by can Doorn & Godefroy (1978), can Doorn (1981) and by Klopman (1994).

These observations seem to justify the use of Equation (8) as the basis of modelling currents in the presence of waves under field conditions and in most laboratory situations.

The present version of the model is open to a number of refinements. First of all with respect to the treatment of the flow above the wave trough. Secondly, the enhancement of the wave Reynolds stress in the presence of a stronger current should be investigated theoretically.

Application of the model above model to surf zone conditions may require adjustments in three areas:

1. An additional term due to bottom slope may need to be added to $\overline{\tilde{u}\tilde{w}}$,
2. A different expression for the flow above the wave trough, e g, a roller model may be needed The eddy viscosity must be enhanced in the upper part of the flow. Guidance in these respects may be found in the measuremetns of Nadaoka & Kondoh (1982) and Cox et al (1995).

The strength of the present model compared with previous ones is that a detailed description is achieved at the bottom at the same time as a reasonable overall water balance. This is of course necessary in order to model natural situations with movable beds.

References

Bijker, EW, JP Th Kalkwijk & T Pieters (1974): Mass transport in gravity waves on a sloping bottom. *Proc 14th Int Conf Coastal Eng*, *ASCE*, pp 447-465.

Coffey, FC & P Nielsen (1986): The influence of waves on current profiles, *Proc 20th Int Conf Coastal Eng, Taipei*, pp 82-96.

Cox, D T, N Kobayashi, & A Okayasu (1995): Experimental and numerical modelling of surf zone hydrodynamics. Research report CACR-95-07, Ocean Engineering Laboratory, University of delaware.

Fredsoe, J (1984): Turbulent boundary layers in wave-current motion. *J Hydraulic Eng*, *ASCE Vol 110, No 8*, pp 1103-1120.

Grant, WD & OS Madsen (1979): Combined wave current interaction with a rough bottom. *J Geophys Res Vol 84 No C4*, pp 1797-1808.

Havinga, FJ (1992): *Sediment concentrations and sediment transport in case of irregular non-breaking waves with a current.* Draft Thesis, Faculty of Civil Engineering, Delft University of Technology.

Heijboer, D (1988): *Zandconcentratie- en stroomsnelheidsverdelingen onder golven en stroom, parts I, II and III,* Delft University of Technology.

Kaaij, Th van der & MWC Nieuwjaar (1987): *Sediment concentrations and sediment transport in case of irregular non-breaking waves with a current, Parts A: Text* 104pp and *Part B: Tables and Figures.* Delft University of Technology, Faculty of Civil Engineering.

Kemp, PH and RR Simons (1982): The interaction between waves and a current: waves propagating with the current. *J Fluid Mech Vol 116,* pp 227-250.

Klopman, G (1994): Vertical structure of the flow due to waves and currents. *Delf Hydraulics Progress Report H 840.30, Part II,* 38pp.

Longuet-Higgins, MS (1953): Mass transport in Water Waves. *Phil Trans Roy Soc Lond, Vol 245 A,* pp 535-581.

Longuet-Higgins, MS (1956): The mechanics of the boundary layer near the bottom in a progressive wave. *Proc 6th Int Conf Coastal Eng, ASCE, Miami,* pp 184-193.

Nadaoka, K & T Kondoh (1982): Laboratory measurements of velocity field structure in the surf zone by LDV. *Coastal Engineering in Japan, Vol 25,* pp 125-146.

Nielsen, P (1985): On the structure of oscillatory boundary layers. *Coastal Engineering, Vol 9,* pp 261-276.

Nielsen, P (1992): *Coastal bottom boundary layers and sediment transport.* World scientific, Singapore, 324pp.

Supharatid, S, H Tanaka & Nshuto (1992): Interactions of waves and current. *Coastal Eng in Japan, Vol 35, No 2,* pp 167-186.

Swan, C (1990): Convection within an experimental wave flume. *J Hydraulic Res, Vol 28, No 3,* pp 273-282.

van Doorn, Th (1981): *Experimental investigation of near-bottom velocities in water waves without and with a current. Report no M 1423 part 1,* Delft Hydraulics, 66pp.

van Doorn, Th & HWHE Godefroy (1978): *Experimental investigation of the bottom boundary layer under periodic progressive water waves. Report no M 1362 part 1,* Delft Hydraulics, 46pp.

Villaret, C and G Perrier (1992): *Transport of fine sand by combined waves and current: An experimental study. Report no HE-42/92.68,* Electricite de France, 81pp.

You, Z-J (1994): A simple model for current velocity profiles in combined wave current flows. *Coastal Engineering, Vol 23,* pp 289-304.